ZnS, ZnSe, and ZnS/ZnSe windows: their impact on FLIR system performance

Claude A. Klein
Bernard diBenedetto
James Pappis
Raytheon Company
Research Division
Lexington, Massachusetts 02173

Abstract. The presence of a solid window at the entrance aperture of an airborne FLIR can degrade the signal-to-noise ratio as a result of (a) the reduction in target signal caused by the absorption of radiation by the window and (b) the loss in system detectivity caused by additional quantum noise generated by window-emitted photons. It is also known that, in order to avoid a degradation of the resolution at spatial frequencies of current interest, the window must satisfy specific requirements in terms of its modulation-transfer characteristics. The purpose of this paper is to consider some relevant properties of chemically vapor-deposited ZnS and ZnSe prior to assessing how windows made from these materials may impact the performance of state-of-the-art FLIRs. The degradation in signal-to-noise ratio occurring in the presence of a ZnS window reflects a substantial increase in absorptance/emittance at the long-wavelength end of the FLIR bandpass (8 to 12 μm) and must be attributed to lattice absorption processes, thus imposing intrinsic limitations on the performance, particularly at elevated temperatures. With ZnSe there is essentially no degradation to be anticipated, but since this material is soft, ZnSe windows cannot cope with rain/ice/dust erosions occurring in an operational environment. This emphasizes the need to develop a "new-generation" FLIR window that combines adequate erosion resistance and ZnSe-type optical properties. The present investigation confirms that ZnS/ZnSe laminates represent a highly attractive solution from the point of view of eliminating the loss of sensitivity encountered with ZnS windows in high speed flight.

Subject terms: infrared optics; FLIR systems; infrared windows; performance degradation; zinc selenide; zinc sulfide; ZnS/ZnSe laminates.

Optical Engineering 25(4), 519-531 (April 1986).

CONTENTS

1. Introduction
2. Key equations
3. ZnS windows
   3.1. Absorption coefficients
   3.2. Thickness requirements
   3.3. Performance degradation
4. ZnSe windows
   4.1. Transmittance/emittance
   4.2. Performance degradation
   4.3. Erosion resistance
5. ZnS/ZnSe windows
   5.1. Spectral transmittance
   5.2. Contrast transmittance
   5.3. Performance degradation
6. Conclusions
7. Acknowledgments
8. Appendix A
9. Appendix B
10. Appendix C
11. Glossary
12. References

Paper 2103 received Jan. 7, 1985; revised manuscript received Oct. 3, 1985; accepted for publication Oct. 23, 1985; received by Managing Editor Nov. 5, 1985.

1. INTRODUCTION

The function of an infrared-transmitting window is to protect thermal imaging equipment such as FLIRs, which operate in the 8 to 12 μm band, against aerodynamic loads as well as rain or dust exposures. The window must perform this function without seriously degrading the nominal performance of the sensor system. This means that (a) the window should not inject significant distortion or loss of resolution in the optical image, (b) the window must transmit useful signal radiation without gross attenuation, and (c) the window should not exhibit much radiance in the wavelength region of system operation, even at the temperatures reached in a high-speed flight environment. In this connection, we emphasize that radiation emanating from aerodynamically heated windows may cause a loss in detectivity, reflecting the additional quantum noise generated by incident window photons. Furthermore, spurious shadings, or "ghosts," may appear if temperature gradients develop on the surface, but this problem can be minimized through careful selection of the window location and will be ignored in this assessment of FLIR-window materials. The primary purpose of the present paper is to outline some relevant concepts and provide essential information on the properties of Raytran ZnS and Raytran ZnSe* in order to evaluate how windows made of these materials, including the newly developed ZnS/ZnSe laminates,[1] can affect the performance of airborne FLIRs.

*Chemically vapor-deposited zinc sulfide and zinc selenide manufactured by Raytheon Company, Research Division, Lexington, Mass.

At this time, germanium is the most widely used FLIR-window material. Germanium exhibits superior mechanical properties but is not suitable for applications involving aerodynamic heating because of excessive free-carrier absorption above room temperature. For instance, sustained flight at altitudes of less than 5000 ft and speeds of no more than Mach 0.8 reduces the transmittance of an AR-coated Ge window from 90% to 60%,[2] which causes an even more severe degradation in signal-to-noise ratio, considering the enhanced background radiation; in effect, Ge windows turn opaque at temperatures approaching 150°C.[3] For applications that require FLIR operation at velocities close to the flight boundary of advanced combat aircraft, as in the case of the Pave Tack system, the window material in current use is chemically vapor-deposited (CVD) ZnS.[4] These windows affect the system performance: Even in a benign environment, structurally sound ZnS windows induce a loss in thermal sensitivity of almost 30%. This loss is caused by intrinsic multiphonon-absorption processes at wavelengths beyond 10.5 μm but remains tolerable over the entire range of anticipated thermal loads; also, CVD-ZnS windows are relatively inexpensive and behave reasonably well in terms of rain-erosion resistance.

Presently contemplated advanced multisensor systems (TV, laser, FLIR) for high performance aircraft call for common-aperture configurations in order to reduce the cost and optimize the design. Accordingly, the window material must possess the following attributes: (a) high transmittance at wavelengths ranging from 0.5 to 12 μm, which also implies the availability of environmentally stable broadband AR coatings, (b) low emittance at temperatures up to 200°C, and (c) adequate resistance to rain erosion and particulate impact. In addition, suitable material should exhibit good "image-spoiling" characteristics in the wavelength region of FLIR operation. None of the available monolithic window materials—halides, semiconductors, or glasses—can satisfy this spectrum of requirements. From an optical point of view, the ideal material is Raytran ZnSe because of its exceptionally low absorption and scatter throughout the 0.5 to 12 μm wavelength range; in terms of system performance, there is essentially no degradation to be anticipated, even at temperatures associated with supersonic flight.[3] This material, however, is too soft and too sensitive to raindrop or solid-particle impingement to be acceptable for use under adverse weather conditions. A logical way to circumvent this inherent limitation is to create a composite structure consisting of a ZnSe substrate thick enough to withstand aerodynamic pressure loads and covered with a sheet of high durability material to provide protection against rain or dust. The concept rests on the premise that sufficient protection can be provided by a thin enough layer of semitransparent but hard material, so that the multispectral capability of the composite will not be impaired; in principle, the joining can be accomplished by direct vapor deposition on ZnSe or by means of a properly chosen bonding agent. Much work has been done along these lines[5–7] for the purpose of selecting a candidate for the protective layer as well as attaching this layer to the substrate.

The solution that best satisfies the need for an erosion-resistant multispectral window amounts to using the CVD process to deposit a thin sheet of ZnS on top of the ZnSe substrate.[8] The selenide surface to be hardened is polished prior to reinserting the plate in the reaction zone of the furnace; after heating to a temperature of about 650°C, ZnS is deposited to the appropriate thickness. In this regard, numerous rain-erosion tests have shown that ZnS layers of no more than 0.5-mm (0.020 in.) thickness can provide a degree of "hardness" comparable to the protection offered by monolithic CVD-ZnS windows. Furthermore, it has been established that such ZnS/ZnSe laminates are structurally sound in the sense that delamination does not occur, even in a dynamic environment, albeit substantial stresses develop upon cooling because of the mismatch in the thermal expansion coefficients. As will be shown in Sec. 5, the optical performance of chemically vapor-deposited ZnS/ZnSe composites is outstanding, especially in the 8 to 12 μm region, and should lead to significant improvements in the context of passive IR applications involving high speed flight. More recently, it has been demonstrated that the manufacturing process can be scaled up, in a cost-effective manner, to produce multispectral ZnS/ZnSe blanks in the sizes required for large-aperture, high-resolution FLIRs.[1]

At this point, we may add that, while it is not the intent of this paper to present a comprehensive discussion of experimental data, the reader should find it convenient to refer to Table I, which lists some key numbers pertaining to mechanical, thermal, and optical properties of standard Raytran ZnS and Raytran ZnSe. We note that both materials are brittle and, therefore, require the use of statistical techniques for a proper characterization of the flexural strength; the numbers in Table I are indicative of average strengths as derived from a large sampling of four-point flexural tests. Absorption coefficients will be considered in Secs. 3 and 4.

First, we must examine how aerodynamically heated windows may affect the performance of a FLIR system (Sec. 2). Following the pattern of an earlier paper,[9] we show that an AR-coated window can degrade the electrical signal-to-noise ratio of airborne FLIRs via two mechanisms: a first-order reduction in target signal caused by radiation absorption in the window and a second-order degradation in system detectivity reflecting the additional quantum noise generated by window photons. In addition, and in order to avoid a loss of resolution in the optical image, the window must satisfy stringent requirements in terms of its spatial transfer characteristics. In this light, we propose to examine the case of monolithic ZnS and monolithic ZnSe in Secs. 3 and 4, re-

TABLE I. Key Properties of Raytran ZnS (standard grade) and Raytran ZnSe, at Room Temperature

	Knoop hardness[a] (kg/mm²)	Flexural strength[a] (psi)	Young's modulus[a] (Mpsi)	Poisson's ratio[a] (1)	Expansion coefficient[b] (°C⁻¹)	Refractive index[c] (1)
Raytran ZnS	250	≃15,000	10.8±0.5	0.29±0.01	7.98×10^{-6}	2.2002
Raytran ZnSe	100	≃ 7,500	10.2±0.4	0.28±0.01	8.57×10^{-6}	2.4065

(a) In-house measurements (Raytheon Research Division, Lexington, Mass.).
(b) Temperature range 20–600°C.[28]
(c) At 10 μm.[15]

spectively; for the purpose of a comparative evaluation, numerical calculations always refer to a 12-in.-diameter circular window, which is subjected to a 1-atm pressure differential, and assume ideal AR coatings. The ZnS/ZnSe laminates will be considered in Sec. 5, where it is shown that they have much to offer in terms of achievable signal-to-noise ratios, particularly at elevated temperatures. The conclusions are stated in Sec. 6; related topics such as pressure-induced distortion, residual surface stresses, and bilayer-transmittance calculations are summarized in the Appendixes.

2. KEY EQUATIONS

The purpose of this section is to provide an analytical base for estimating the degradation in FLIR-system performance that may result from the presence of a material window at the entrance aperture. In this regard, we note that the minimum-resolvable-temperature-difference (MRT) concept provides an excellent measure of the performance of a FLIR system, with or without the window, because it is indicative of the thermal sensitivity as well as the limiting resolution at high spatial frequencies. For our purposes, the MRT function is best expressed as follows[10]:

$$\mathrm{MRT}(f_T) = 3\,\frac{\mathrm{NET}}{\mathrm{MTF}(f_T)}\left(\frac{\bar{\rho} f_T \bar{\beta}}{t_e \dot{F}}\right)^{1/2}, \tag{1}$$

where f_T designates the target spatial frequency, NET is the noise-equivalent temperature difference, and MTF represents the overall modulation transfer function of the system; the other symbols are as identified in the Glossary (Sec. 11) but do not concern us here because they refer to parameters that are independent of the presence of a window.

We now proceed to consider how the presence of a window may alter the system's MRT as formulated in Eq. (1). For this purpose, we recall that the NET is defined as that temperature difference between two large adjacent blackbody sources near room temperature that produces a signal-to-noise ratio of unity in the electrical "image" of the transition between the two sources. In other words, since

$$\mathrm{NET} \equiv \frac{\Delta T}{\mathrm{SNR}} \tag{2}$$

and since the window induces a degradation in signal-to-noise ratio, there will be a loss in thermal sensitivity reflected by an increase in the system's NET:

$$(\mathrm{NET})_W = \frac{(\mathrm{NET})_O}{(\mathrm{SNR})_W/(\mathrm{SNR})_O}. \tag{3}$$

In the same vein, since the system's MTF includes contributions originating from the various components, with

$$\mathrm{MTF} \equiv \prod_{k=1}^{n} \tilde{r}_k, \tag{4}$$

it is immediately seen that the MTF of a "bare" system must be multiplied by the transfer function of the window in order to arrive at an overall modulation transfer function:

$$(\mathrm{MTF})_W = \tilde{r}_W(\mathrm{MTF})_O. \tag{5}$$

This assumes, of course, that scattering and other image-spoiling properties of the window material can be characterized by means of a line spread function, thus establishing the precise effect of a specific blank on the optical system.[11] On this basis, we conclude that, in the presence of an external window, the performance of a FLIR can be described by means of a modified MRT function,

$$(\mathrm{MRT})_W = \frac{(\mathrm{MRT})_O}{[(\mathrm{SNR})_W/(\mathrm{SNR})_O]\tilde{r}_W}, \tag{6}$$

which properly combines the MRT of the bare system, the window-induced degradation in signal-to-noise ratio, and the window-related contribution to spatial transfer characteristics.

At this point, it should be mentioned that the degradation in signal-to-noise ratio can be evaluated in rather general terms, as specific features of the optical arrangement other than those relating to the spectral band of system operation do not enter the calculation. In Ref. 3, we have shown that, for systems operating in a photon-noise-limited mode, difficulties arising in evaluating the signal-to-noise ratio in the presence of a "hot window" can be avoided by considering an SNR defined as the ratio of H_{eff} and NEI, where H_{eff} represents an effective signal irradiance for extended targets and NEI is the noise-equivalent irradiance at the peak-response wavelength of the detector. In this manner, it is seen that the degradation involves a reduction in target signal and an increase in system noise:

$$\frac{(\mathrm{SNR})_W}{(\mathrm{SNR})_O} = \frac{(H_{eff})_W/(H_{eff})_O}{(\mathrm{NEI})_W/(\mathrm{NEI})_O}. \tag{7}$$

Considering the purpose of the present analysis, we may postulate spectrally averaged atmospheric loss factors,* which leads to

$$\frac{(H_{eff})_W}{(H_{eff})_O} = \frac{\int_{\lambda_1}^{\lambda_2} T(\lambda, T_W) W_\lambda(T_B)\, d\lambda}{\int_{\lambda_1}^{\lambda_2} W_\lambda(T_B)\, d\lambda}, \tag{8}$$

where $T(\lambda, T_W)$ measures the transmittance of the window and $W_\lambda(T_B)$ is the spectral radiant exitance of the background scene. If, in addition, we assume that (a) the window is at a uniform temperature and exhibits Lambertian characteristics, (b) the detector package includes a cold shield, which is fully effective in blocking extraneous noise, and (c) the optics including the detector entrance window exhibits little absorption throughout the wavelength region of detec-

*Amlin's attempt to incorporate the effects of atmospheric attenuation and radiance in an analysis of this type (Ref. 6) refers to a specific system and appears to be in need of revision (see Ref. 12).

tor response, it turns out that[9]

$$\frac{(\mathrm{NEI})_W}{(\mathrm{NEI})_O} = \left[\frac{\int_{\lambda_1}^{\lambda_2} E(\lambda, T_W) Q_\lambda(T_W)\, d\lambda + \int_{\lambda_1}^{\lambda_2} T(\lambda, T_W) Q_\lambda(T_B)\, d\lambda}{\int_{\lambda_1}^{\lambda_2} Q_\lambda(T_B)\, d\lambda} \right]^{1/2} . \tag{9}$$

Here $E(\lambda, T_W)$ is the window emittance, whereas $Q_\lambda(T_W)$ and $Q_\lambda(T_B)$ refer to the spectral quantum exitance of the window and the background, respectively. We conclude that, for most situations of practical interest, Eqs. (7) through (9) provide a simple and elegant formalism for assessing the degradation in signal-to-noise ratio resulting from the presence of a hot window at the entrance aperture of a passive IR sensor. Furthermore, these equations clearly identify the material properties that enter the analysis, that is, the emittance and the transmittance, which stresses the importance of obtaining accurate absorption coefficients at wavelengths and temperatures of system relevance. In Secs. 3 through 5, we perform this task for ZnS, ZnSe, and ZnS/ZnSe windows, which should allow us to assess the system-sensitivity degradation in a straightforward manner, once the integrals in Eqs. (8) and (9) have been evaluated.

3. ZnS WINDOWS

For applications involving substantial aerodynamic heating, Raytran ZnS is the preferred "interim" FLIR-window material because it can cope with the rain-erosion problem and can be produced in large sizes at an acceptable cost. In this section, we will consider in some detail how ZnS windows degrade the performance of an operational FLIR system (Sec. 3.3); this requires not only accurate information on the absorption coefficient at the wavelengths and temperatures of interest (Sec. 3.1), but also some understanding of the factors that determine the thickness of the window (Sec. 3.2). In this context, we will attempt to throw light on the issue of pressure-induced optical distortion and its impact on required window thicknesses [Appendix A (Sec. 8)].

3.1. Absorption coefficients

The room-temperature transmittances listed in Table II reflect the results (average and standard deviation) of measurements performed on 93 0.2-in.-thick specimens originating from 9 ZnS deposition runs. These measurements, which were carried out on a Perkin-Elmer Model 580 B ratio-recording infrared spectrophotometer, reveal that there is some nonuniformity in the 8 to 12 μm transmittance, even among samples cut from the same deposit. An illustration of the distribution can be seen in Fig. 1, which refers to the transmittance at 10 μm.

TABLE II. Infrared Transmittance and Absorption Coefficient of Standard-Grade Raytran ZnS (uncertainties reflect standard deviations)

Wavelength (μm)	Transmittance[a] (%)	Absorption coeff. (cm^{-1})
8	72.05 ± 0.81	0.072 ± 0.022
9	71.99 ± 0.48	0.079 ± 0.013
10	71.61 ± 0.41	0.096 ± 0.011
11	61.56 ± 0.43	0.393 ± 0.013
12	61.64 ± 0.49	0.400 ± 0.016

(a) Thickness: 0.51 cm (0.2 in.)

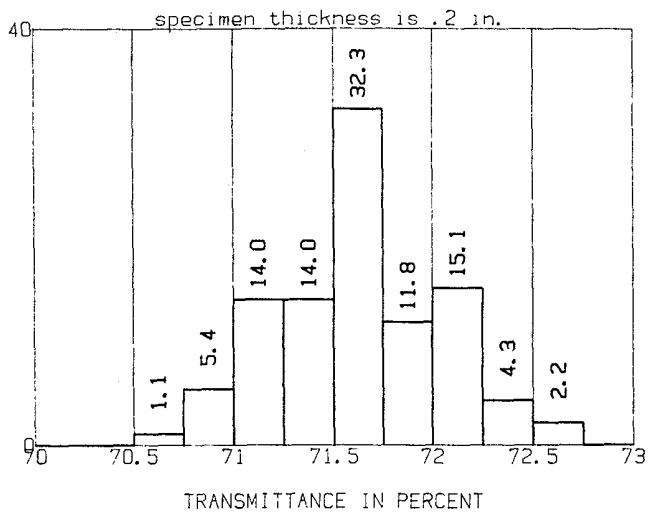

Fig. 1. Distribution (in percent) of the measured room-temperature transmittance of Raytran ZnS at 10 μm.

The transmittance of an optical blank is determined by the combination of surface losses and losses caused by volume as well as surface absorption. For near-normal incidence, and in the absence of interference effects, the classic expression for the transmittance is

$$T = \frac{(1-R)^2 \exp(-\beta t)}{1 - R^2 \exp(-2\beta t)} , \tag{10}$$

which takes multiple internal reflections into account. The absorption coefficient β may then be derived from the measured transmittance:

$$\beta = \frac{1}{t} \ln \left\{ \frac{(1-R)^2}{2T} + \left[R^2 + \frac{(1-R)^4}{4T^2} \right]^{1/2} \right\} , \tag{11}$$

if the single-surface reflectivity R is available. Previously, it was shown that, in the wavelength range of FLIR operation, not only does scatter play an insignificant role, but the extinction coefficient remains much smaller than the refractive index[13]; it follows that the reflectivity R of uncoated ZnS is simply

$$R = \frac{(n-1)^2}{(n+1)^2} . \tag{12}$$

With an index as given by Dodge,[14]

$$n^2 = 1 + \sum_{i=1}^{3} \frac{A_i \lambda^2}{\lambda^2 - \lambda_i^2} , \tag{13}$$

where A_i and λ_i are empirically determined constants obtained through fitting to a three-term Sellmeier dispersion relation, Eq. (11) then yields the room-temperature absorp-

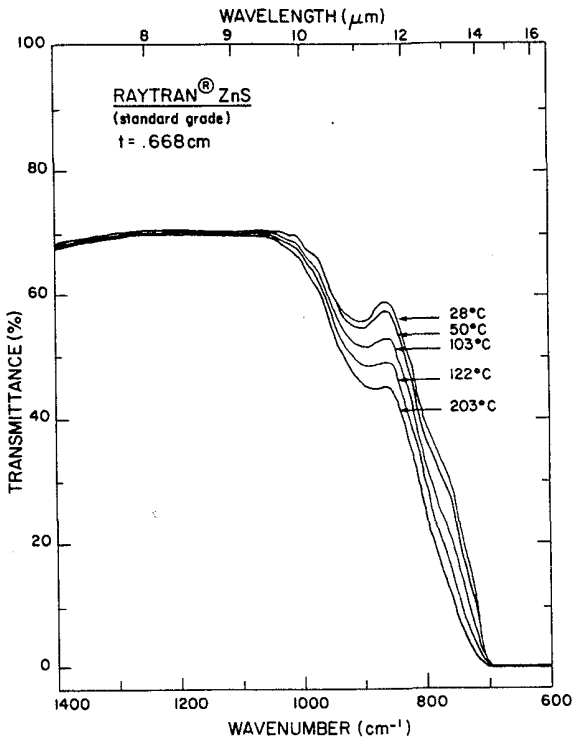

Fig. 2. Spectral transmittance of Raytran ZnS at elevated temperatures.

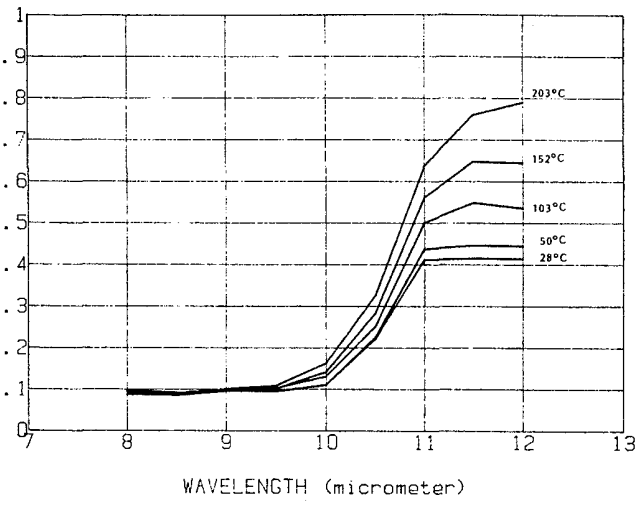

Fig. 3. Absorption coefficient (1/cm) of Raytran ZnS at elevated temperatures.

tion coefficients listed in Table II. In this connection, we note that, for $\lambda \lesssim 10$ μm, the absorption is weak, and the transmittance becomes essentially a function of the reflectivity; this in turn implies that a proper application of Eq. (11) assumes correct inputs in terms of the refractive index.

Above room temperature, the long-wavelength transmittance of Raytran ZnS exhibits a pattern as displayed in Fig. 2, which concerns a 0.67-cm-thick specimen of standard material. Beyond 9.5 μm, the transmittance becomes temperature sensitive and falls off at a rate that is indicative of multiphonon-excitation mechanisms; the strong absorption band at 885 cm^{-1} (11.3 μm), in particular, can be attributed to TO overtones and is seen to shift toward longer wavelengths as the temperature increases.[13] This mode-softening phenomenon confirms the intrinsic nature of the absorption and, by the same token, points to inherent limitations on the performance of ZnS windows in a FLIR application. For the purpose of obtaining absorption coefficients, we take it that the semiempirical expression of Li,[15]

$$n^2(\lambda, T) = \epsilon_0(T) + \frac{A(T)}{\lambda^2 - \lambda_U^2(T)} + \frac{\epsilon_0(T) - \epsilon_\infty(T)}{[\lambda/\lambda_I(T)]^2 - 1}, \tag{14}$$

gives a correct description of the index and its spectral dependence at temperatures as in Fig. 2. At a fixed temperature, Eq. (14) boils down to a Sellmeier-type dispersion with λ_U and λ_I referring to the fundamental edge in the UV and the IR, respectively; at a given wavelength, however, the temperature dependence reflects that of the two dielectric constants, which, *faute de mieux*, Li expresses as a fourth-order polynomial.[15] On this basis, and in conjunction with Eqs. (11) and (12), the transmittance traces recorded in Fig. 2 yield absorption coefficients as plotted in Fig. 3. This procedure clearly demonstrates that, above 10 μm, the absorption is a strong function of both wavelength and temperature; in effect, the absorption increases with temperature in an almost exponential manner, which is as anticipated in a phonon-dominated regime and in accord with previous observations based on 10.6 μm calorimetry.[13] At shorter wavelengths ($8 \lesssim \lambda \lesssim 9.5$ μm), there is no evidence of spectral features or temperature-activated events, which emphasizes the dominance of impurities in the absorption process. Finally, and in conjunction with Fig. 3, it should be mentioned that, for the purpose of doing machine calculations, we found it convenient to use an analytical representation of the bivariate function $\beta(\lambda, T)$,

$$\beta(\lambda, T) = \sum_{i=0}^{4} \lambda^i \left(\sum_{j=0}^{2} c_{ij} T^j \right), \tag{15}$$

and thus reproduce the actual absorption coefficients with an error of less than 1%.

3.2. Thickness requirements

In addition to meeting systems requirements with respect to signal-to-noise ratios and modulation transfer characteristics, FLIR windows must satisfy structural requirements stemming from the mechanics of high speed flight. Specifically, the window must withstand dynamic pressures amounting to[16]

$$\Delta p = (0.7) p_\infty M_\infty^2 \tag{16}$$

in air; at low altitudes and top speeds of Mach 1.2,[3] the window must therefore withstand uniform pressure loadings of approximately one atmosphere (14.7 psi). As stated earlier (Sec. 1), in this paper it is postulated that the window will be subjected to a differential pressure of no more than the commonly encountered 1 atm specification.

Consider now the case of a circular window simply sup-

ported at its outer edge.* The maximum bending moment then occurs at the center of the window, and the corresponding stress is[17]

$$\sigma_{max} = \frac{3(3+\nu)}{8}\frac{\Delta p(D/2)^2}{t^2}, \tag{17}$$

where ν refers to Poisson's ratio; since ν is close to 0.3 for both ZnS and ZnSe, it follows that we may rewrite Eq. (17) as

$$\sigma_{max} = (0.309)\Delta p\left(\frac{D}{t}\right)^2. \tag{18}$$

According to conventional brittle-material design practice, the allowable tensile stress should not exceed a peak value of

$$\sigma_p \leqslant \frac{\sigma_f}{SF} \tag{19}$$

if σ_f is the nominal fracture strength and SF represents a safety factor preferably set equal to 4. On making use of Eqs. (18) and (19), it is therefore a simple matter to derive an analytical expression for the thickness of a "safe" window. In order to avoid catastrophic failure, the window must have an aspect ratio t/D equal to or larger than the limiting aspect ratio for fracture,

$$\frac{t_f}{D} = 0.556\left(\frac{\Delta p}{\sigma_f/SF}\right)^{1/2}. \tag{20}$$

Since $\Delta p = 14.7$ psi and $\sigma_f = 15$ kpsi, it is seen that a 12-in. (30-cm) diameter chemically vapor-deposited ZnS window must have a minimum thickness of 0.42 in. or 1.1 cm.

Pressure-induced optical distortion[18] should also be considered as a potentially limiting factor because the pressure deforms the window, causing it to turn into a "lens" with a finite focal length and higher-order aberrations. In Appendix A (Sec. 8), we show that there will be no undue optical distortion if the aspect ratio of the window is at least equal to

$$\frac{t_d}{D} = 0.513\left[(n-1)\left(\frac{\Delta p}{E}\right)^2\left(\frac{D}{\lambda}\right)\right]^{1/5}, \tag{21}$$

which suggests that the size of the window controls the "weight" of pressure-induced distortions. In effect, it follows from Eqs. (20) and (21) that the "critical diameter," or diameter at which optical and mechanical failure are of equal import in terms of required window thicknesses, amounts to

$$D_o = 1.45\sqrt{\Delta p}\,E^2\left(\frac{SF}{\sigma_f}\right)^{5/2}\left(\frac{\lambda}{n-1}\right) \tag{22}$$

and, thus, that fracture is the primary failure mode for $D < D_o$. On inserting property values as listed in Table I, the reader will easily convince himself that, for the situations of interest here, pressure-induced distortion is an irrelevant factor in prescribing window thicknesses.

3.3. Performance degradation

Returning now to Eq. (6), and keeping in mind that Raytran ZnS windows do not seem to affect the contrast transmittance of an MTF test apparatus, even at spatial frequencies as high as 20 cycles/mrad,[13] we take it that the increase in MRT caused by the presence of a ZnS window at the entrance aperture of a FLIR system results in a performance degradation best "measured" by the ratio

$$\frac{(MRT)_O}{(MRT)_W} = \frac{(SNR)_W}{(SNR)_O}. \tag{23}$$

The task on hand thus amounts to evaluating the reduction in target signal [Eq. (8)] and the increase in system noise [Eq. (9)] as a function of the window temperature. For the sake of convenience, we are assuming that the window has fully effective AR coatings in the spectral band of system operation. This implies that the transmittance of the "case window" is

$$T(\lambda, T_W) = \exp[-\beta(\lambda, T_W)t], \tag{24}$$

where t = 1.1 cm and β is as obtained from Eq. (15)†; similarly, under thermal equilibrium conditions, the emittance reduces to

$$E(\lambda, T_W) = 1 - \exp[-\beta(\lambda, T_W)t]. \tag{25}$$

The two spectral exitances

$$W_\lambda(T) = \frac{3.7418 \times 10^4\ \mathrm{W \cdot \mu m^4 \cdot cm^{-2}}}{\lambda^5[\exp(c_2/\lambda T) - 1]} \tag{26}$$

and

$$Q_\lambda(T) = \frac{1.8831 \times 10^{23}\ \mathrm{\mu m^3 \cdot cm^{-2} \cdot s^{-1}}}{\lambda^4[\exp(c_2/\lambda T) - 1]}, \tag{27}$$

where $c_2 = 1.4388 \times 10^4$ μm · K if λ and T are in micrometers and degrees Kelvin, respectively. The task thus boils down to performing a sequence of numerical integrations over the system's bandpass (λ_1, λ_2 = 8, 12 μm) at discrete window temperatures ranging from 20° to 200°C, and a steady background at 295 K. The results are displayed in Fig. 4 and demonstrate that the degradation in system performance caused by a 1.1-cm (0.43-in.) thick ZnS window is indeed serious. The degradation increases almost linearly with window temperature from about 20% in a room-temperature environment to 50% or more in supersonic flight.

4. ZnSe WINDOWS

The development of chemically vapor-deposited ZnSe windows was carried out in the framework of the CO_2 high-

*In other words, assume that the window frame interacts with the window itself essentially in the manner of a simple support since this corresponds to a worst case, in terms of thickness requirements.

†A listing of the 15 c_{ij} will be provided upon request.

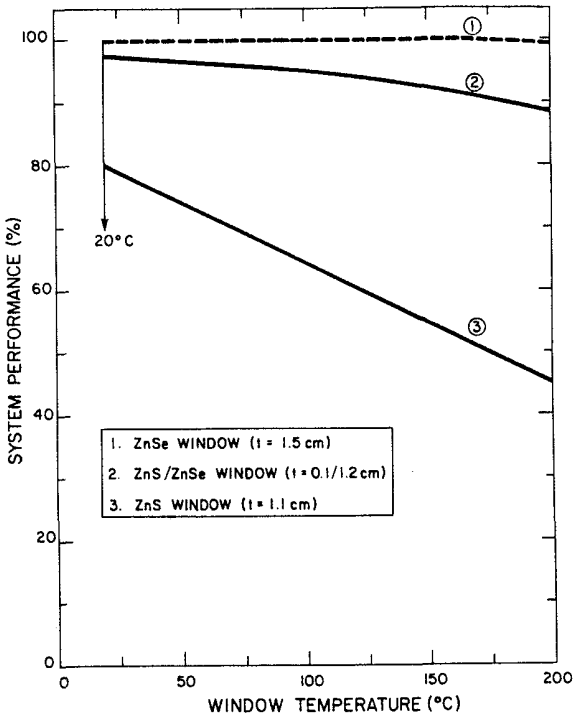

Fig. 4. Relative FLIR-system performance as a function of the window temperature, for three CVD material candidates. The thicknesses reflect requirements associated with a 30-cm-diameter aperture and a 1-atm uniform pressure load. Note that ZnSe windows are "for illustration only," considering their inadequate resistance to rain erosion.

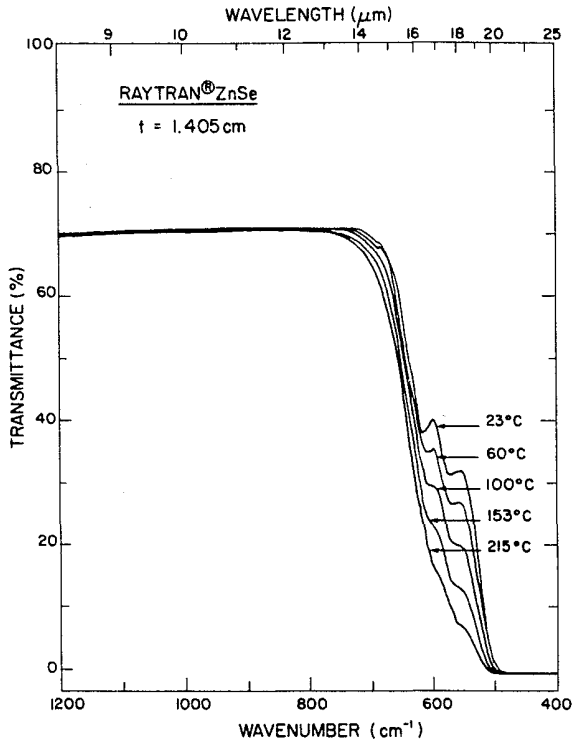

Fig. 5. Spectral transmittance of Raytran ZnSe at elevated temperatures.

energy laser effort and culminated in the creation of an optical ceramic with exceptional properties in the 8 to 12 μm wavelength region (Sec. 4.1). In principle, FLIR windows made of ZnSe do not degrade the performance of the sensor system (Sec. 4.2) but cannot be used in an operational environment because of the rain-erosion situation. In Sec. 4.3, we will review this problem and take advantage of the discussion to consider the desirability of developing a "hardened" product such as laminated ZnS/ZnSe composites.

4.1. Transmittance/emittance

The long-wavelength transmittance of a 1.405-cm-thick piece of Raytran ZnSe, at temperatures ranging from 23° to 215°C, is illustrated in Fig. 5. Considering the objective of the present investigation, we note that, below 12 μm, there is virtually no change with temperature, which is in accord with earlier work using 10.6 μm calorimetry at elevated temperatures.[19] We also note that throughout the 8 to 12 μm wavelength region, an application of the zero-absorption theoretical transmittance law,

$$T = \frac{2n}{n^2 + 1}, \tag{28}$$

yields essentially the same numbers as recorded on the spectrophotometer chart; at 10 μm, for instance, the refractive index is 2.406,[15] which yields T = 0.709, in accord with the measured transmittance of 71%, at room temperature.

Since standard spectrophotometric measurements cannot be relied on to generate accurate values of the absorption in CVD ZnSe at the wavelengths of interest, it should be advantageous to turn to emittance techniques, as demonstrated in Fig. 6. This figure displays the 7 to 14 μm emittance spectrum of a 0.45-cm-thick specimen of Raytran ZnSe at 80 and 370 K; and since the emittance is of the order of 1% or less, Fig. 6 also reflects the behavior of the absorption coefficient, keeping in mind that the relation

$$E = \beta t \tag{29}$$

then holds. Perhaps most striking is the reversal in the nature of the temperature dependence, which strongly suggests that, above 12.5 μm and in accord with Fig. 5, the absorption is dominated by low-multiplicity phonon processes, whereas at shorter wavelengths the temperature dependence is indicative of "residual" molecular impurities. The strong band at approximately 9.25 μm ($\simeq 1080\ cm^{-1}$), in particular, may be due to ZnO formed when the material is allowed to remain in air for long periods of time.[20] Other workers report that typical absorption coefficients at wavelengths of less than 11 μm lie in the range 3 to 10×10^{-4} cm^{-1}.[21] For our purposes, we take it that, between 20° and 200°C, the absorption coefficient of Raytran ZnSe is independent of temperature and equal to $1 \times 10^{-3}\ cm^{-1}$, from 8 to 11 μm, but rises to $5 \times 10^{-3}\ cm^{-1}$ at 12 μm, as suggested in Fig. 6.

4.2. Performance degradation

For the sake of completeness, we now apply the procedure of Sec. 3.3 to the case of a CVD-ZnSe window of 1.5-cm thickness designed to withstand a pressure load of 1 atm in a 30-cm-diameter geometry. With temperature-independent absorption coefficients, Eq. (15) reduces to

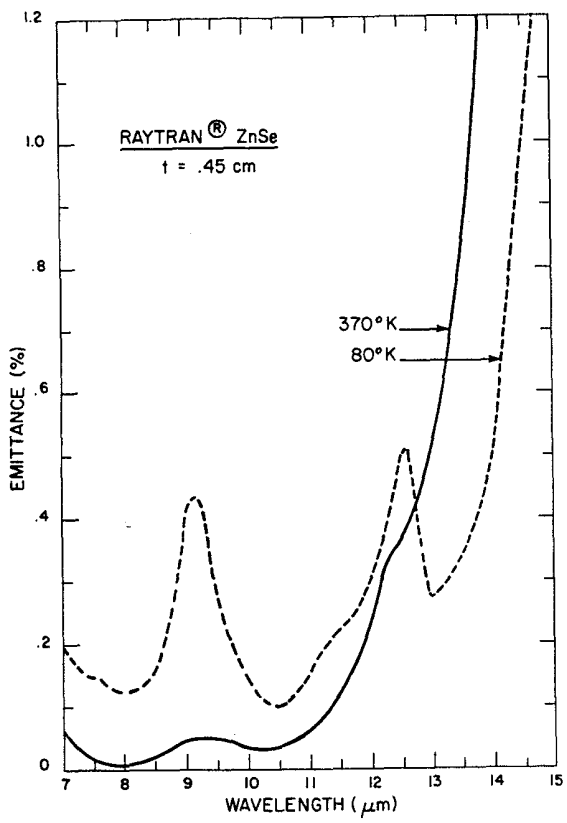

Fig. 6. Spectral emittance of Raytran ZnSe (measurements by D. Stierwalt, Naval Electronics Lab., Corona, Calif.).

$$\beta(\lambda) = \sum_{i=0}^{4} c_i \lambda^i \tag{30}$$

and, thus, allows for a simpler algorithm. The results are displayed in Fig. 4 and confirm that, in principle, there is no detectable degradation to be anticipated with ZnSe windows[3]; note, however, the trend at temperatures in excess of 150°C, which must be attributed to the photon noise originating from the hot window [see Eq. (9)].

4.3. Erosion resistance

Infrared-transmitting windows made of brittle material are subject to damage and loss of transmittance when exposed to rain in a high velocity environment. The mechanisms that cause "erosion" as a result of multiple raindrop impacts are fairly complex[22] but are believed to involve two essential steps: (1) the development of a network of internal fractures that may extend to significant depths* and are triggered by the high tensile stresses generated when a raindrop hits the surface, and (2) the removal of a finite amount of material, which may occur in conjunction with the rapid lateral outflow of liquid that escapes from the impact zone. The ability of monolithic window material to withstand rain erosion thus directly relates to the fracture strength as well as the surface hardness. The threshold velocity, in particular,

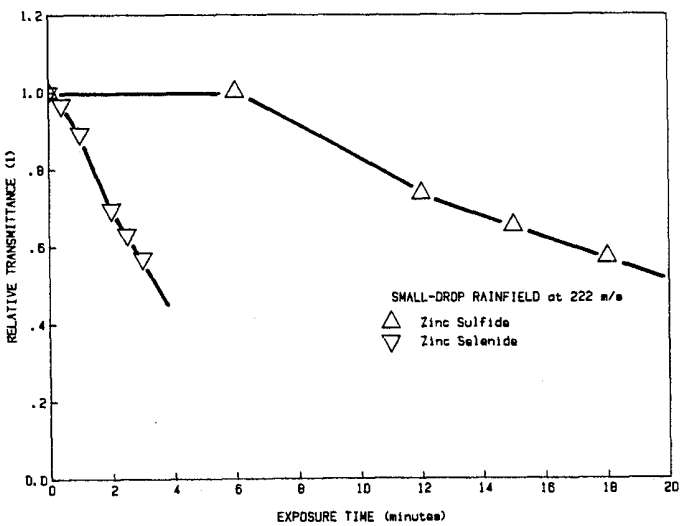

Fig. 7. A comparison of the rain-erosion resistance of CVD ZnS and CVD ZnSe. The small-drop rain field is made up of 0.75-mm-diameter water drops falling at the rate of 1 cm/h. Data taken from Ref. 24.

or velocity at which a complete ring-fracture pattern emerges, should be a function of the intrinsic fracture toughness and the ability of the crystal lattice to resist microcrack propagation.

The case of chemically vapor-deposited ZnS and ZnSe is perhaps best discussed in the light of Fig. 7, which is based on data collected at the AFML/Bell facility[24] and illustrates the severity of the rain-erosion problem in ZnSe. The loss of transmittance at long wavelengths must be attributed, initially, to reflections at internal fracture surfaces rather than scatter caused by surface pits. With ZnS, on the contrary, there is an "incubation period" during which the 10 μm transmittance does not seem to be adversely affected; significant degradation occurs only in conjunction with the nucleation and growth of erosion pits on the surface.

At this point, it is recalled (Sec. 1) that the most successful approach to hardening CVD ZnSe consists in depositing a layer of ZnS on the exposed surface. Such ZnS/ZnSe "laminates" exhibit essentially the same erosion resistance as monolithic CVD ZnS if the thickness of the protective layer is of the order of 50 mil or more; zinc sulfide layers of 20 mil or less do not buy much protection because the cracks then tend to propagate into the selenide substrate.† It has also been reported that ZnS/ZnSe composites with ZnS layers of between 0.030- and 0.050-in. thickness tested "better" than specimens with thicker coatings, in the sense that crack propagation appeared to be inhibited.[8] One possible explanation assumes a residual compressive stress in the ZnS layer, which would increase the magnitude of the radial tensile loadings that can be sustained. Indeed, since the coefficient of thermal expansion for ZnSe is greater than for ZnS (see Table I) and since a stress-free condition is believed to exist at the deposition temperature, the mismatch in thermal expansion should give rise to compressive stresses as the composite cools down. As shown in Appendix B (Sec. 9), these stresses decrease when the thickness of the coating in-

*This is why broadband antireflective coatings, which are usually less than 5 μm thick, cannot be expected to improve the rain-erosion resistance of window materials.[23]

†T. Peterson, Private communication (AFML, Dayton, Ohio, 1979).

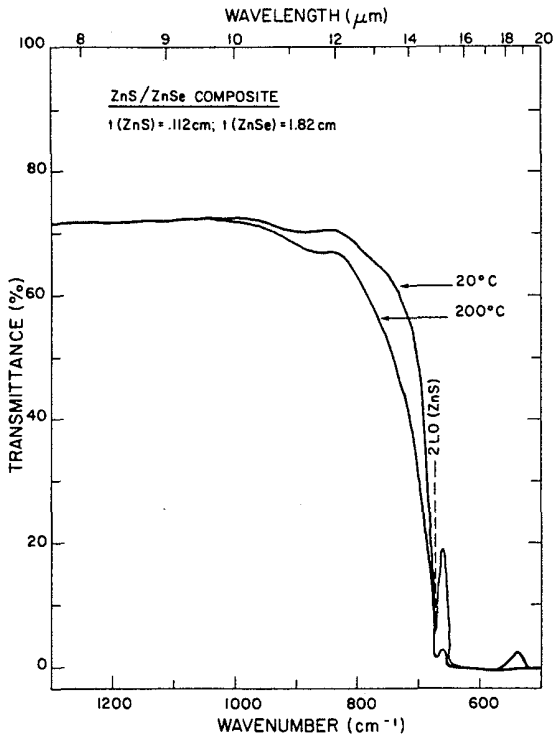

Fig. 8. Spectral transmittance of a ZnS/ZnSe laminated window blank at two temperatures.

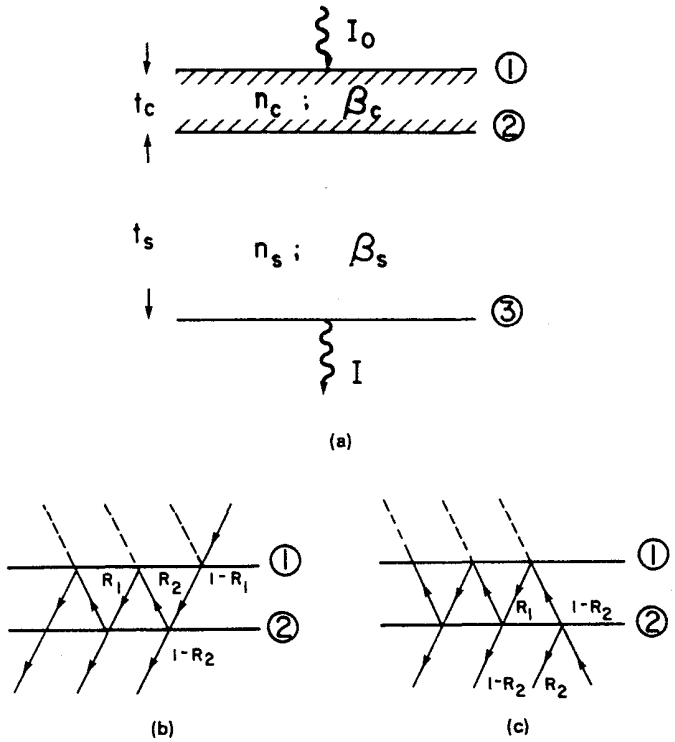

Fig. 9. A model for evaluating the transmittance of a bilayered composite window.

creases, which is consistent with the rain-erosion resistance behavior, keeping in mind that a minimum coating thickness is required to confine the damage to the ZnS layer.

5. ZnS/ZnSe WINDOWS

Composite FLIR windows of current interest consist of a highly transparent substrate (CVD ZnSe) thick enough to withstand aerodynamic pressure loads and covered with a layer of directly deposited ZnS; rain-erosion testing (Sec. 4.3) indicates that, for best results, this layer should be approximately 1 mm thick. In this section, we first consider experimental and analytical results on the optical behavior of such laminates in the 8 to 12 μm wavelength region: specifically, the spectral transmittance (Sec. 5.1) and the contrast transmittance (Sec. 5.2). In Sec. 5.3, it is then demonstrated that ZnS/ZnSe laminates offer significant improvements in terms of FLIR performance.

5.1. Spectral transmittance

The long-wavelength transmittance of a typical composite is illustrated in Fig. 8, which displays the multiphonon "tailing off" at two temperatures, 20° and 200°C. The presence of the ZnS causes the transmittance to exhibit some temperature dependence starting at approximately 11 μm (3TO≃ 885 cm^{-1}) and accounts for the sharp cutoff beyond 14 μm, which must be attributed to a two-phonon excitation process that has been assigned to the ZnS LO branch (2LO ≃ 660 cm^{-1}).[25] Of some concern is the matter of the interface, which calls for a rigorous analysis if one wishes to assess the impact of interface imperfections on the overall behavior of laminated ZnS/ZnSe structures.

In Appendix C (Sec. 10), it is shown that the model presented in Fig. 9, which assigns the subscript c to the ZnS coating and the subscript s to the ZnSe substrate, leads to the following expression for the transmittance of a bilayered optical blank:

$$T = \frac{(1-R_1)(1-R_2)(1-R_3)\exp(-\beta_c t_c - \beta_s t_s)}{1 - R_1R_2\exp(-2\beta_c t_c) - R_2R_3\exp(-2\beta_s t_s) - R_1R_3(1-2R_2)\exp(-2\beta_c t_c - 2\beta_s t_s)}, \quad (31)$$

where the single-surface reflectivities are

$$R_1 = \frac{(1-n_c)^2}{(1+n_c)^2}, \quad R_2 = \frac{(n_c-n_s)^2}{(n_c+n_s)^2}, \quad R_3 = \frac{(n_s-1)^2}{(n_s+1)^2}. \quad (32)$$

On using Li's wavelength- and temperature-dependent expressions for the two indices,[15] in conjunction with absorption coefficients as derived from Eq. (15) for ZnS and Eq. (30) for ZnSe, it is a straightforward matter to write a computer code that outputs the transmittance of the composite at any wavelength λ and temperature T of interest ($8 \leq \lambda \leq 12$ μm, $20°C \leq T \leq 200°C$). Some significant results are given in Table III and compared with data read off Fig. 8 at both 20° and 200°C; the transmittance of the composite is seen to be almost exactly as predicted, thus establishing the quality of the product as well as the validity of the analysis.

TABLE III. Measured and Calculated Transmittance of a ZnS/ZnSe Laminated Window Blank*

Wavelength (μm)	Temperature (°C)	Transmittance(%) Measured	Calculated
8	20	71.2	71.6
	200	71.0	71.4
9	20	71.7	71.8
	200	71.3	71.5
10	20	72.0	72.0
	200	71.5	71.2
11	20	70.0	69.8
	200	67.8	67.6
12	20	70.0	69.4
	200	66.2	66.2

*t(ZnS) = 0.044 in. (0.11 cm); t(ZnSe) = 0.716 in. (1.82 cm)

5.2. Contrast transmittance

From the point of view of FLIR imaging applications, it remains to be established that chemically vapor-deposited ZnS/ZnSe blanks are indeed acceptable in terms of the modulation transfer function (MTF) at wavelengths ranging from 8 to 12 μm. In this regard, it is recalled that the performance of an optical system is best described by means of a line spread function (LSF) because it yields the transfer function, or contrast transmittance, simply by taking the Fourier transform[10]:

$$\mathrm{MTF} = F\{\mathrm{LSF}\}. \tag{33}$$

As evidenced in Fig. 10, the presence of a full-size (14 in. × 18 in.) composite plate at the entrance aperture of our line-scan test apparatus does not have a significant effect on the MTF of the system, at the spatial frequencies of interest; note that advanced FLIRs have nominal resolutions of 0.1 mrad in the narrow field-of-view mode,[26] which implies that they do not respond to spatial frequencies beyond a limit of 10 cycles/mrad.

5.3. Performance degradation

Since state-of-the-art ZnS/ZnSe composite windows do not inject a significant reduction in MTF, it follows that any window-induced degradation in overall system performance must result from a loss in signal-to-noise ratio, as outlined in Sec. 2. An evaluation of this loss requires correct expressions for the transmittance as well as the emittance of the composite window. In this regard, and since we are assuming fully effective AR coatings, that is, $R_1 = R_3 = 0$, Eq. (31) immediately tells us that the window transmittance as a function of wavelength and temperature should be

$$\mathbf{T}(\lambda, T_W) = [1 - R_2(\lambda, T_W)]\exp[-\beta_c(\lambda, T_W)t_c - \beta_s(\lambda, T_W)t_s], \tag{34}$$

where the subscripts c and s refer to the ZnS coating and the ZnSe substrate, respectively; the reflectivity R_2 is as given in Eq. (32) and can be expressed as a function of wavelength and temperature by means of the semiempirical equations of Li[15] for the two indices. An evaluation of the emittance requires some care because

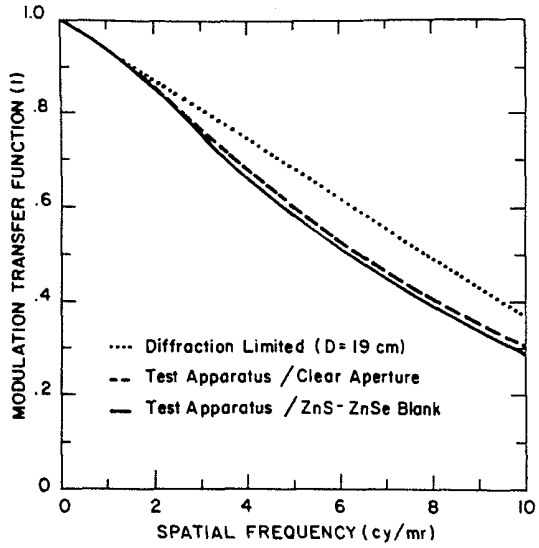

Fig. 10. Contrast transmittance of the Raytheon MTF test apparatus, with and without window.

$$\mathbf{E}(\lambda, T_W) = 1 - \mathbf{R}(\lambda, T_W) - \mathbf{T}(\lambda, T_W) \tag{35}$$

and AR coatings cannot suppress additional reflections originating from the ZnS/ZnSe interface. The fraction of incident light that is reflected as a result of the presence of the interface is immediately seen to be

$$\mathbf{R}(\lambda, T_W) = R_2(\lambda, T_W)\exp[-2\beta_c(\lambda, T_W)t_c], \tag{36}$$

which leads to the conclusion that the emittance $\mathbf{E}(\lambda, T_W)$ that is to be inserted into the noise-enhancement equation [Eq. (9)] must be expressed as in Eq. (35) with **R** and **T** as in Eqs. (36) and (34), respectively. The two absorption coefficients, of course, should be as in Eqs. (15) and (30).

In a dynamic environment, the pressure loads on a composite window are such that the ZnSe surface will be placed in tension. Flexural tests conducted in this geometry indicate that the nominal fracture strength of the composite is of the order of 10 kpsi.[1] In this light, and if D = 12 in. and Δp = 1 atm, as postulated for our model system, the minimum thickness of the composite window should be 0.51 in. (1.30 cm), which suggests that t_c = 0.040 in. (0.1 cm) and t_s = 0.47 in. (1.20 cm) are "good" numbers to use in the context of assessing the performance of ZnS/ZnSe composite windows. The results of numerical calculations that were carried out in accord with this scheme, for radiant and quantum exitances as specified earlier, are displayed in Fig. 4. It is seen that the degradation in performance caused by ZnS/ZnSe composite windows should be minimal; even at temperatures as high as 200°C, and for moderately performing AR coatings, both target-detection and target-recognition ranges should be barely affected. In this sense, the present investigation confirms that ZnS/ZnSe composite windows represent highly attractive solutions from the point of view of eliminating, or reducing, the loss of sensitivity encountered with first- and second-generation (Ge and ZnS) FLIR windows in a high-speed flight environment.

6. CONCLUSIONS

Chemical vapor deposition of ZnS yields a credible FLIR-window material for advanced combat aircraft. This material remains transparent in the 8 to 12 μm wavelength region, at elevated temperatures; it exhibits adequate resistance to rain erosion; and it can be produced in large sizes, at an acceptable cost. Accurate information is now available on the index of refraction and the coefficient of absorption, at wavelengths and temperatures of current interest. The degradation in system performance induced by ZnS windows reflects both the phonon-dominated absorption of target radiation and the emission of noise radiation that occur at the long-wavelength end of the FLIR bandpass. These mechanisms can give rise to a 50% increase in minimum resolvable temperature, under environmental conditions that are representative of the flight boundary.

The development of chemically vapor-deposited ZnSe for high-energy laser windows has stimulated interest in assessing the capabilities of this material in a FLIR application. The optical performance of ZnSe in the long-wavelength IR was shown to be outstanding; poor rain-erosion resistance, however, rules out the use of monolithic ZnSe windows in an operational environment. In this regard, the successful development of large ZnS/ZnSe laminated window blanks represents a major step forward.

In Sec. 5.1, it is demonstrated that the infrared properties of ZnS/ZnSe composites are as predicted for a "perfect" interface. Operation in a true "multispectral" mode may thus be anticipated. With regard to FLIR performance, laminated ZnS/ZnSe composites offer significant improvements in the sense that the degradation in signal-to-noise ratio caused by ZnS phonons is largely eliminated; in addition, the rain-erosion resistance appears to be enhanced by compressional stresses resulting from the mismatch of the expansion coefficients. Further calculations must be performed to ascertain the advantage of using ZnS/ZnSe composite windows under conditions such that atmospheric attenuation becomes an essential factor in terms of overall signal-to-noise ratios.[12]

7. ACKNOWLEDGMENTS

This work was performed, in part, under Contract No. F33615-80-C-5013 monitored by AFML/AFWAL/AFSC.

8. APPENDIX A

The deflection of a uniformly loaded, elastically isotropic, and simply supported circular window obeys an equation such as

$$w(r) = \frac{3\Delta p(1-\nu^2)}{16Et^3}\left[\frac{5+\nu}{1+\nu}\left(\frac{D}{2}\right)^2 - r^2\right]\left[\left(\frac{D}{2}\right)^2 - r^2\right], \quad \text{(A-1)}$$

as long as the displacements are small compared to the thickness.[17] On introducing a dimensionless radial variable

$$\rho = \frac{r}{D/2} \quad \text{(A-2)}$$

and setting ν equal to 0.3, Eq. (A-1) becomes

$$w(\rho) = 0.0107\left(\frac{\Delta p D^4}{Et^3}\right)(4.08 - \rho^2)(1-\rho^2), \quad \text{(A-3)}$$

which shows that the deflection "scales" with the fourth power of the diameter. Sparks and Cottis[18] demonstrate that, for small deflections, the optical path difference at normal incidence is

$$\mathrm{OPD} = \frac{t}{2}(n-1)\left(\frac{dw}{dr}\right)^2, \quad \text{(A-4)}$$

which yields

$$\mathrm{OPD} = 3.66 \times 10^{-3}\left[\frac{(n-1)\Delta p^2 D^6}{E^2 t^5}\right](2.54 - \rho^2)^2\rho^2 \quad \text{(A-5)}$$

if the deflection is as in Eq. (A-3). The pressure-induced change in optical path length is thus seen to be a strong function of the aspect ratio of the window, t/D, and to generate wavefront deformations involving a simple shift of the image as well as third- and fifth-order spherical aberrations. Since the deformation is fairly smooth, the Rayleigh limit, $(\mathrm{OPD})_{max} \leq \lambda/4$, applies and should provide a reliable criterion for assessing the tolerable aberration:

$$(\mathrm{OPD})_{max} = 8.89 \times 10^{-3}\left[\frac{(n-1)\Delta p^2 D^6}{E^2 t^5}\right], \quad \text{(A-6)}$$

which suggests that the distortion will remain tolerable if the aspect ratio of the window is at least equal to

$$\frac{t_d}{D} = 0.513\left[(n-1)\left(\frac{\Delta p}{E}\right)^2\left(\frac{D}{\lambda}\right)\right]^{1/5}. \quad \text{(A-7)}$$

The functional dependence turns out to be the same as that obtained in Ref. 18 by means of a different procedure, but the numerical coefficient differs substantially in the sense that our result points to thinner nondistorting windows.

9. APPENDIX B

A composite window blank fabricated by chemically vapor-depositing ZnS on a ZnSe plate deforms into a spherical surface when its temperature T differs from the temperature T_o at which the deposition was made. This deformation, if caused by a mismatch in expansion coefficients, is accompanied by flexural stresses in the two materials. On assuming that a stress-free condition exists at the deposition temperature, the residual stress in the top surface of the coating is[27]

$$\sigma_c = -\frac{K_2}{K_1}\frac{(\alpha_s - \alpha_c)(T - T_o)E_c}{1 - \nu_c}, \quad \text{(B-1)}$$

where K_1 and K_2 are two dimensionless factors; since Poisson's ratios of ZnS and ZnSe are almost identical, and on introducing the parameters $\gamma = E_c/E_s$ and $\delta = t_c/t_s$ for the moduli and the thicknesses, these factors reduce to

$$K_1 = 4 + 6\delta + 4\delta^2 + \gamma\delta^3 + \frac{1}{\gamma\delta} \quad \text{(B-2)}$$

and

$$K_2 = 3\delta + 2\delta^2 - \frac{1}{\gamma\delta}. \quad \text{(B-3)}$$

In-house measurements, as well as work done at the University of Dayton,[28] indicate that, over the relevant temperature range ($T = 20°C$, $T_o = 650°C$), the difference in expansion corresponds to a difference in expansion coefficients, $\alpha_s - \alpha_c$, of about $0.6 \times 10^{-6}\,°C^{-1}$. On this basis, we find that a chemically vapor-deposited laminate made of a ZnSe substrate and a ZnS layer having thicknesses of 0.510 in. and 0.034 in., respectively, should exhibit residual compressive stresses of 4,250 psi in the top surface. In fact, strain measurements that were carried out on such a structure confirm that the ZnS layer was in compression, at a level of about 3,000 psi, and almost independently of the position.[8]

10. APPENDIX C

Consider a situation as illustrated in Fig. 9(a) and assume that the thickness of the coating is much greater than the wavelength of the incident radiation; in other words, assume that there is no phase coherence between multireflected internal rays. If T_c is the transmittance of the coating and R_c' its reflectance for light incident from the substrate, the total transmittance is[29]

$$T = \frac{T_c T_3 \exp(-\beta_s t_s)}{1 - R_3 R_c' \exp(-2\beta_s t_s)}, \tag{C-1}$$

where T_3 and R_3 denote the transmissivity and the reflectivity of the backface. Since the coating is made up of a single layer of homogeneous material, the summation of transmitted [Fig. 9(b)] and reflected [Fig. 9(c)] intensities yields

$$T_c = \frac{(1 - R_1)(1 - R_2)\exp(-\beta_c t_c)}{1 - R_1 R_2 \exp(-2\beta_c t_c)} \tag{C-2}$$

and

$$R_c' = \frac{R_2 + R_1(1 - 2R_2)\exp(-2\beta_c t_c)}{1 - R_1 R_2 \exp(-2\beta_c t_c)}, \tag{C-3}$$

respectively. Returning now to Eq. (C-1), and keeping in mind that $T_3 = 1 - R_3$, it is seen that

$$T_c T_3 \exp(-\beta_s t_s) = \frac{(1 - R_1)(1 - R_2)(1 - R_3)\exp(-\beta_c t_c - \beta_s t_s)}{1 - R_1 R_2 \exp(-2\beta_c t_c)} \tag{C-4}$$

and

$$1 - R_3 R_c' \exp(-2\beta_s t_s) = \frac{1 - R_1 R_2 \exp(-2\beta_c t_c) - R_2 R_3 \exp(-2\beta_s t_s) - R_1 R_3 (1 - 2R_2)\exp(-2\beta_c t_c - 2\beta_s t_s)}{1 - R_1 R_2 \exp(-2\beta_c t_c)}. \tag{C-5}$$

It follows that the correct expression for the transmittance of a laminated window blank, at normal incidence, is as given in Eq. (31) with single-surface reflectivities as in Eq. (32), for weakly absorbing materials. Prior analytical assessments of ZnS/ZnSe composite windows[1] made use of

$$T \simeq \frac{(1 - R_1)(1 - R_2)(1 - R_3)\exp(-\beta_c t_c)}{1 - R_2 R_3 - R_1(R_2 + R_3 - 2R_2 R_3)\exp(-2\beta_c t_c)}, \tag{C-6}$$

which holds only if the absorptance of the substrate can be neglected compared to the absorptance of the coating ($\beta_s t_s << \beta_c t_c$); in effect, Eq. (C-6) applies only to relatively thin composites with highly transparent substrates.

11. GLOSSARY

A	:	empirical constant
c_2	:	second radiation constant
c_{ij}	:	set of coefficients
D	:	window diameter
D_o	:	critical diameter
$\mathbf{E}$	:	window emittance
E	:	modulus of elasticity
$\dot{F}$	:	frame rate
f_T	:	target spatial frequency
H_{eff}	:	effective signal irradiance
K	:	dimensionless factor
M_∞	:	Mach number
n	:	refractive index
p_∞	:	free-stream pressure
Q_λ	:	spectral quantum exitance
$\mathbf{R}$	:	window reflectance
R	:	single-surface reflectivity
r	:	radial variable
$\tilde{r}_W$	:	window transfer function
$\mathbf{T}$	:	window transmittance
T_B	:	background temperature
T_o	:	deposition temperature
T_W	:	window temperature
t	:	window thickness
t_d	:	limiting thickness, distortion
t_e	:	eye integration time
t_f	:	limiting thickness, fracture
W_λ	:	spectral radiant exitance
w	:	displacement/deflection
α	:	expansion coefficient
β	:	absorption coefficient
$\bar{\beta}$	:	vertical subtense
γ	:	modulus ratio, E_c/E_s
Δp	:	differential pressure
ΔT	:	temperature increment
δ	:	thickness ratio, t_c/t_s
ϵ_o	:	static dielectric constant
ϵ_∞	:	optical dielectric constant
λ	:	radiation wavelength
λ_I	:	IR absorption edge
λ_U	:	UV absorption edge
ν	:	Poisson's ratio
ρ	:	dimensionless radial variable
$\bar{\rho}$	:	bandwidth ratio
σ	:	mechanical stress
σ_f	:	fracture strength
σ_{max}	:	maximum stress
σ_p	:	tolerable peak stress
LSF	:	line spread function
MRT	:	minimum resolvable temperature difference
MTF	:	modulation transfer function

NET : noise-equivalent temperature difference
OPD : optical path difference
SNR : signal-to-noise ratio
$()_O$: "no window"
$()_W$: "with window"

12. REFERENCES

1. J. Pappis and B. diBenedetto, "ZnS/ZnSe sandwich-type FLIR windows," Report No. AFWAL-TR-83-4122, AFML (1983).
2. H. Hafner and G. Cronin, "Development of gallium arsenide for infrared windows," Report No. AFML-TR-75-49 (1975).
3. C. Klein, "FLIR window materials for advanced combat aircraft: their impact on system sensitivity," in *Proc. 1976 IRIS Meeting on Infrared Imaging*, p. 37 (1976).
4. D. Amlin, "Degradation in FLIR sensitivity due to window absorptance/emittance," Report No. ASD/ENA-79-6, Aeronautical Systems Division, WPAFB, Ohio (1979).
5. W. Kramer, R. Hopkins, G. Brandt, R. Hoffman, J. Schruben, and K. Steinbruegge, "Development of multispectral sandwich-type IR windows," Report No. AFML-TR-77-53 (1977).
6. A. Swanson, P. Miles, and J. Pappis, "Chemically vapor-deposited semiconductors for laser and infrared window applications," Report No. AFML-TR-77-34 (1977).
7. R. Tustison, "Erosion-resistant FLIR window materials," Report No. AFWAL-TR-80-4199 (1980).
8. R. Donadio, J. Connolly, and J. Pappis, "Sandwich-type FLIR windows," Report No. AFML-TR-79-4113 (1979).
9. C. Klein, J. Pappis, and B. diBenedetto, "Chemical vapor-deposited zinc sulfide windows and FLIR system performance," in *Proc. 1977 IRIS Meeting on Infrared Imaging*, p. 185 (1977).
10. M. Lloyd, *Thermal Imaging Systems*, Chap. 5, Plenum Publishing Co., New York (1975).
11. C. Reynolds, "Image spoiling properties of selected materials for the infrared," Infrared Physics 8, 233 (1968).
12. C. Klein, "Can ZnS/ZnSe laminated windows improve the performance of the PAVE TACK FLIR?" in *Proc. 1985 IRIS Meeting on Infrared Imaging*, p. 149 (1985).
13. C. Klein, B. diBenedetto, R. Donadio, T. Kohane, and J. Pappis, "Lattice absorption, phonon assignments, and image-spoiling properties of CVD ZnS in the infrared," in *Laser-Induced Damage in Optical Materials: 1978*, Nat. Bur. Stand. (U.S.) Spec. Publ. 541, p. 86 (1979).
14. M. Dodge, "Refractive properties of CVD zinc sulfide," in *Laser-Induced Damage in Optical Materials: 1977*, Nat. Bur. Stand. (U.S.) Spec. Publ. 509, p. 83 (1978).
15. H. Li, "Refractive index of ZnS, ZnSe, and ZnTe and its wavelength and temperature derivatives," CINDAS Report 64, Purdue Univ. (1982).
16. L. Prandtl, *Führer durch die Strömungslehre*, Chap. 2, F. Vieweg, Braunschweig (1956).
17. S. Timoshenko and W. Krieger, *Theory of Plates and Shells*, Chap. 3, McGraw Hill, New York (1959).
18. M. Sparks and M. Cottis, "Pressure-induced optical distortion in laser windows," J. Appl. Phys. 44, 787 (1973).
19. L. Skolnik, H. Lipson, B. Bendow, and J. Schott, "Temperature dependence of the absorption coefficient of GaAs and ZnSe at 10.6 μm," Appl. Phys. Letters 25, 442 (1974).
20. H. Lipson, "Impurity absorption in CVD ZnSe," Appl. Optics 16, 2902 (1977).
21. P. Miles, J. Pappis, and R. Tustison, "Synthesis and characterization of infrared transmitting materials," Report No. AFOSR-TR-81-0251 (1981).
22. W. F. Adler, "Degradation of optical materials exposed to erosive environments," in *Scattering in Optical Materials*, S. Musikant, ed., Proc. SPIE 362, 116 (1983).
23. W. W. Doerffler, W. T. Boord, and H. Y. B. Mar, "Rain erosion-resistant antireflective coatings for infrared windows," in *Optics in Adverse Environments*, E. Bernal G and H. V. Winsor, eds., Proc. SPIE 121, 170 (1978).
24. V. Hackworth and L. Kocher, "Behavior of infrared window materials exposed to rain-drop environments at velocities of 2000 fps (610 m/s)," Report No. AFML-TR-78-184 (1978).
25. C. Klein and R. Donadio, "Infrared active phonons in cubic zinc sulfide," J. Appl. Phys. 51, 797 (1980).
26. R. Siwechi and L. Neznanski, "Test results of the AN/AAQ-9 (PAVE TACK FLIR)," in *Proc. 1978 IRIS Meeting on Infrared Imaging*, p. 9 (1978).
27. R. Roark and W. Young, *Formulas for Stress and Strain*, Chap. 10, McGraw Hill, New York (1975).
28. G. Graves, J. Wimmer, and W. McCullum, "Exploratory development on multidisciplinary characterization of infrared transmitting materials," Report No. AFML-TR-79-4152 (1979).
29. O. Heavens, *Optical Properties of Thin Solid Films*, Chap. 4, Academic Press, New York (1955).